DALTON

Macrocyclic dimeric vanadium(IV) and heterodinuclear vanadium(IV)–nickel(II) complexes. Structure, magnetic, electronic and redox properties †

Sasankasekhar Mohanta,[a] Kausik K. Nanda,[a] Soma Ghosh,[b] Monika Mukherjee,[b] Madeleine Helliwell[c] and Kamalaksha Nag*,[a]

[a] *Department of Inorganic Chemistry, Indian Association for the Cultivation of Science, Calcutta 700 032, India*
[b] *Department of Solid State Physics, Indian Association for the Cultivation of Science, Calcutta 700 032, India*
[c] *Department of Chemistry, University of Manchester, Manchester M13 9PL, UK*

The oxovanadium(IV) complexes $[\{VO(H_2L^1)\}_2(\mu\text{-}SO_4)][NO_3]_2$, $[(VO)L^1Ni(H_2O)_2(SO_4)]\cdot H_2O$ and $[(VO)L^1Ni(\mu\text{-}SO_4)(H_2O)]\cdot 2H_2O$ have been synthesized from the dinucleating tetraaminodiphenol macrocycle H_2L^1. The crystal structure of the first, in which two unco-ordinated amino nitrogens are protonated, has been determined. The two distorted-octahedral vanadium centres in the complex, separated by 6.741(4) Å, are bridged by sulfate and have an *anti*-oxo configuration. In the solid state the magnetic moment of this complex per vanadium decreases from 1.71 to 1.64 μ_B on lowering the temperature from 299 to 5 K, indicating very weak intra-/or inter-molecular exchange interactions. Its ESR spectra in fluid solution and glass, however, showed the absence of VO • • • VO electron-spin interaction. This complex undergoes stepwise oxidation to produce $VO^{IV}VO^{V}$ and $VO^{V}VO^{V}$ species with $E_{\frac{1}{2}}(1) = 0.445$ V and $E_{\frac{1}{2}}(2) = 0.60$ V *vs.* Ag–AgCl electrode; the comproportionation constant $K_c = 4.2 \times 10^2$. The other two complexes have identical composition but differ in their IR and UV/VIS spectra and electrochemistry. In the first the oxovanadium(IV) and nickel(II) centres are reversibly oxidized at 0.436 and 0.756 V, respectively, while in the second irreversible oxidation of both metal centres takes place at 1.05 and 1.25 V. Both behave ferromagnetically and their exchange coupling constants J are 10(1) and 6(1) cm^{-1}, respectively.

In a recent publication[1] we have reported the chemistry of mononuclear VO^{VI}, heterodinuclear $VO^{IV}Ni^{II}$ and heterotrinuclear $VO^{IV}Ni^{II}VO_2^{V}$ complexes of the dinucleating macrocyclic ligand H_2L^2. The unequal cavity sizes of the two compartments of H_2L^2 were exploited to produce positional and geometrical isomers. Earlier, we reported[2] the structure and magnetic properties of the homodinuclear oxovanadium(IV) complex $[(VO)_2L^1(\mu\text{-}SO_4)]\cdot MeOH\cdot 3H_2O$ of the symmetrical macrocyclic ligand H_2L^1. We now report additional chemistry of several more heterodinuclear oxovanadium(IV) complexes of H_2L^1 and the structure of yet another sulfato-bridged complex $[\{VO(H_2L^1)\}_2(\mu\text{-}SO_4)][NO_3]_2$, in which the two metal centres are held wide apart. The synthesis of heteronuclear oxovanadium(IV) complexes is directed towards evolving ferromagnetic materials by involving orthogonal magnetic orbitals of the interacting metal ions.[3]

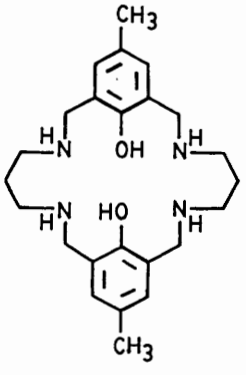

H_2L^1

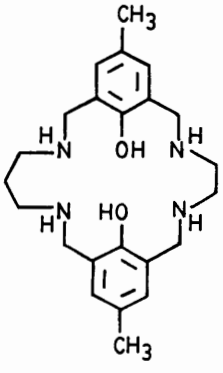

H_2L^2

Experimental

Materials

The compound H_2L^1 was prepared as reported earlier.[4] The acetylacetonates $[VO(acac)_2]$, $[Ni(acac)_2]$[5] and $[VO(H_2L^1)(SO_4)]\cdot 3H_2O$ **2**[2] were obtained according to literature methods. All chemicals were obtained from commercial sources and used as received.

Synthesis

$[VO(L^1)]\cdot H_2O$ 1. This compound was prepared[2] earlier in 40% yield by treating $[VO(OEt)_3]$ with H_2L^1. A much improved yield can be obtained in the following way. To a refluxing methanol solution (100 cm^3) of H_2L^1 (1.65 g, 4 mmol) was added $[VO(acac)_2]$ (1.06 g, 4 mmol). Initially a red solution was obtained, from which eventually orange crystals of **1** began to separate. After 1 h of reflux the product was filtered off, washed with methanol and dried in air; yield 1.65 g (84%).

$[\{VO(H_2L^1)\}_2(\mu\text{-}SO_4)][NO_3]_2$ 3. Complex **2** (0.63 g, 1 mmol) was stirred in methanol (50 cm^3) and finely ground $Pb(NO_3)_2$ (1.66 g, 0.5 mmol) was added in small instalments. After stirring the mixture for 1 h the $PbSO_4$ that precipitated was filtered off. The red filtrate was reduced to *ca.* 10 cm^3 on a rotary evaporator and an equal volume of acetonitrile was added. The solution was kept overnight at room temperature, during which time compound **3** deposited as violet crystals. It was filtered off, washed with acetonitrile and dried in air; yield 0.35 g (60%) (Found: C, 48.5; H, 6.15; N, 11.75. $C_{48}H_{72}N_{10}O_{16}SV_2$ requires

† *Non-SI unit employed:* $\mu_B \approx 9.27 \times 10^{-24}$ J T^{-1}.

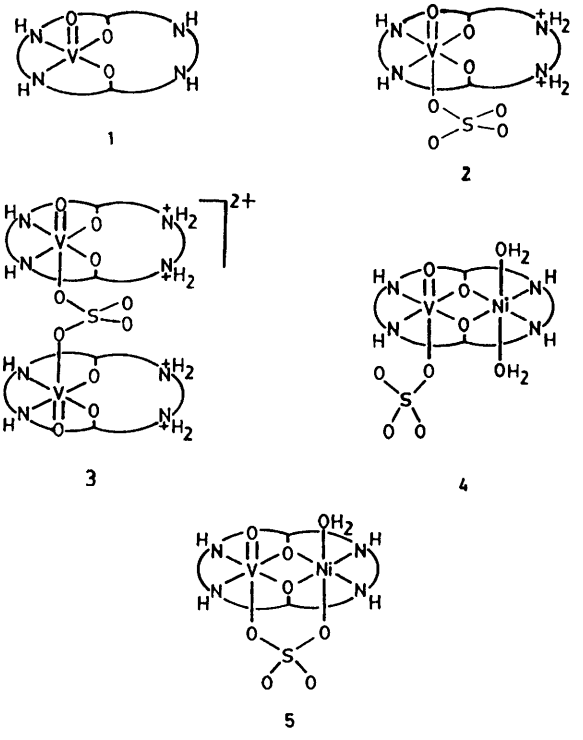

C, 48.9; H, 6.1; N, 11.9%). $\tilde{\nu}/cm^{-1}$ (KBr) 3260w [ν(NH)], 2850w, 2780w [$\nu(NH_2^+)$], 1615m [δ(NH)], 1385s, 830m [$\nu(NO_3^-)$], 1210m, 1170m, 1125s, 1030m, 625m, 610m [$\nu(SO_4^{2-})$] and 955s [ν(V=O)]. λ_{max}/nm ($\varepsilon/dm^3\ mol^{-1}\ cm^{-1}$) (MeOH) 820 (60), 525 (175) and 295 (17 400).

[(VO)L¹Ni(H₂O)₂(SO₄)]·H₂O 4. A mixture of compound **2** (0.63 g, 1 mmol) and [Ni(acac)₂] (0.26 g, 1 mmol) in methanol (50 cm^3) was refluxed for 1 h. The resulting red-violet solution was filtered to remove any remaining solid and the filtrate then rotary evaporated to a pasty mass. On adding acetone (30 cm^3) and stirring, solidification of the pasty mass occurred, and it was filtered off and washed with chloroform. The product on recrystallization from acetonitrile–methanol (1:1) afforded purple crystals; yield 0.51 g (75%) (Found: C, 41.8; H, 5.7; N, 8.3. $C_{24}H_{40}N_4NiO_{10}SV$ requires C, 42.0; H, 5.85; N, 8.15%). $\tilde{\nu}/cm^{-1}$ (KBr) 3260w [ν(NH)], 1625m [δ(NH)], 1180s, 1060m, 630m, 610m [$\nu(SO_4^{2-})$] and 975s [ν(V=O)]. λ_{max}/nm ($\varepsilon/dm^3\ mol^{-1}\ cm^{-1}$) (MeOH) 1140 (5), 780 (20), 520 (45) and 295 (6850).

[(VO)L¹Ni(μ-SO₄)(H₂O)]·2H₂O 5. To a stirred suspension of compound **1** (0.49 g, 1 mmol) in methanol (25 cm^3) was added an aqueous solution (5 cm^3) of $NiSO_4 \cdot 6H_2O$ (0.26 g, 1 mmol). After 0.5 h the wine-red solution that had formed was filtered and the filtrate slowly concentrated on a hot-plate. The violet crystals which separated were filtered off; yield 0.58 g (85%) (Found: C, 41.7; H, 5.95; N, 7.95. $C_{24}H_{40}N_4NiO_{10}SV$ requires C, 42.0; H, 5.85; N, 8.15%). $\tilde{\nu}/cm^{-1}$ (KBr) 3240m [ν(NH)], 1620m [δ(NH)], 1230s, 1180s, 1120s, 1060m, 990m, 625m, 605m [$\nu(SO_4^{2-})$] and 950s [ν(V=O)]; λ_{max}/nm ($\varepsilon/dm^3\ mol^{-1}\ cm^{-1}$) (MeOH) 1120 (10), 710 (30), 680 (32), 570 (sh) (15), 470 (55) and 350 (125).

Physical measurements

Infrared spectra were recorded on a Perkin-Elmer 783 spectrophotometer using KBr discs, UV/VIS and near-IR spectra on a Shimadzu UV-160A or Hitachi U3400 spectrometer and X-band ESR spectra on a Varian E-109C spectrometer using diphenylpicrylhydrazyl (dpph, $g = 2.0037$) as the calibrant. Electrochemical measurements were performed with a BAS 100B system. A standard three-electrode configuration was used, with platinum working and auxiliary electrodes and a Ag–AgCl reference electrode. The supporting electrolyte was tetraethylammonium perchlorate (0.1 mol dm^{-3}) and all solutions were *ca.* 1 mmol dm^{-3} in complex. Variable-temperature magnetic susceptibility measurements were carried out either by using a PAR 155 vibrating-sample magnetometer (85–300 K) or a Faraday balance[6] (5–300 K). Diamagnetic corrections were made using Pascal's constants. The C, H and N analyses were performed on a Perkin-Elmer 2400 II elemental analyser.

Crystallography

Crystals suitable for structure determination of compound **3** were obtained by diffusing diethyl ether into a solution of it in acetonitrile–methanol (1:1). Intensity data were collected with a Rigaku AFC5R diffractometer at 293 K using graphite-monochromated Cu-Kα radiation ($\lambda = 1.5418$ Å). Pertinent crystallographic data are summarized in Table 1. The cell parameters were obtained by least-squares refinement of twenty automatically centred reflections. Three standard reflections were monitored after every 150 during data collection and no significant variations in intensities were observed. The intensity data were corrected for Lorentz-polarization effects and for absorption by an empirical method.[7]

The structure was solved by the Patterson heavy-atom method (SHELX 76)[8] and refined by full-matrix least-squares techniques on F^2 using the program SHELXL 93.[9] All the non-hydrogen atoms, except the two disordered oxygen atoms of the two nitrate ions, which were treated isotropically, were refined anisotropically. The hydrogen atoms located either from Fourier-difference maps or placed at their geometrically calculated positions were held fixed during refinement. The atomic scattering factors were taken from ref. 10. The refinement converged to $R1 = 0.077$ and $wR2 = 0.173$ and the difference map showed ripples ranging between +0.41 and −0.33 e $Å^{-3}$.

Atomic coordinates, thermal parameters, and bond lengths and angles have been deposited at the Cambridge Crystallographic Data Centre (CCDC). See Instructions for Authors, *J. Chem. Soc., Dalton Trans.*, 1996, Issue 1. Any request to the CCDC for this material should quote the full literature citation and the reference number 186/202.

Results and Discussion

Synthesis and characterization

The macrocycle H_2L^1 reacts almost quantitatively with $[VO(acac)_2]$ to produce $[VO(L^1)]\cdot H_2O$ **1**. As reported earlier, **1** is practically insoluble in common organic solvents and is characterized by a strong V=O stretch at 855 cm^{-1}. The synthesis and characterization of the protonated mononuclear oxovanadium(IV) complex $[VO(H_2L^1)(SO_4)]\cdot 3H_2O$ **2** have been reported[2] and its structure seems to be similar to that determined for $[VO(H_2L^2)(SO_4)]\cdot 5H_2O$,[11] in which the vanadium occupies the N_2O_2 equatorial plane provided by the larger compartment of the ligand and the unidentate sulfate is *trans* to the vanadyl oxygen, while the two unco-ordinated amine nitrogens of the vacant ligand compartment are protonated. A metathetical reaction between 2 equivalents of **2** and 1 equivalent of lead nitrate produces a violet complex of composition $[\{VO(H_2L^1)\}_2(\mu\text{-}SO_4)][NO_3]_2$ **3**. The IR spectrum exhibits, in addition to the ligand NH stretching at 3260 cm^{-1}, two bands at 2850 and 2780 cm^{-1} due to the protonated amine stretchings. The presence of bridging sulfate in **3** has been inferred from a cluster of bands due to co-ordinated sulfate at 1210, 1170, 1125 and 1030 cm^{-1} [$\nu_3(SO_4^{2-})$] and at 625 and 610 cm^{-1} [$\nu_4(SO_4^{2-})$]. Further, the two strong bands at 1385 and 830 cm^{-1} indicate the presence of ionic nitrate. The terminal

Table 1 Crystallographic data for $[\{VO(H_2L^1)\}_2(\mu\text{-}SO_4)][NO_3]_2$ **3**

Formula	$C_{48}H_{72}N_{10}O_{16}SV_2$
M	1179.1
Crystal colour	Violet
Crystal size/mm	0.28 × 0.26 × 0.23
Crystal system	Monoclinic
Space group	$P2_1/n$
a/Å	12.562(2)
b/Å	23.602(5)
c/Å	19.017(4)
β/°	101.63(2)
U/Å^3	5523(2)
Z	4
D_c/g cm^{-3}	1.42
Scan mode	ω–2θ
μ(Cu-Kα)/cm^{-1}	38.3
$F(000)$	2480
$2\theta_{max}$/°	102
Reflections measured	5944
Unique reflections	5755
Reflections with $I > 3\sigma(I)$	2947
Parameters refined	696
$R1(F)$[a]	0.077
$wR2(F^2)$[b]	0.173
S[c]	1.36

[a] $R1(F) = \Sigma||F_o| - |F_c||/\Sigma|F_o|$. [b] $wR2(F^2) = [\Sigma w(F_o^2 - F_c^2)^2/\Sigma w(F_o^2)^2]^{\frac{1}{2}}$ where $w = 1/[\sigma^2(F_o^2) + (0.0489P)^2 + 26.12P]$ and $P = (F_o^2 + 2F_c^2)/3$. [c] $S = [\Sigma w(F_o^2 - F_c^2)^2/(N - P)]^{\frac{1}{2}}$ where N is the number of data and P the total number of parameters refined.

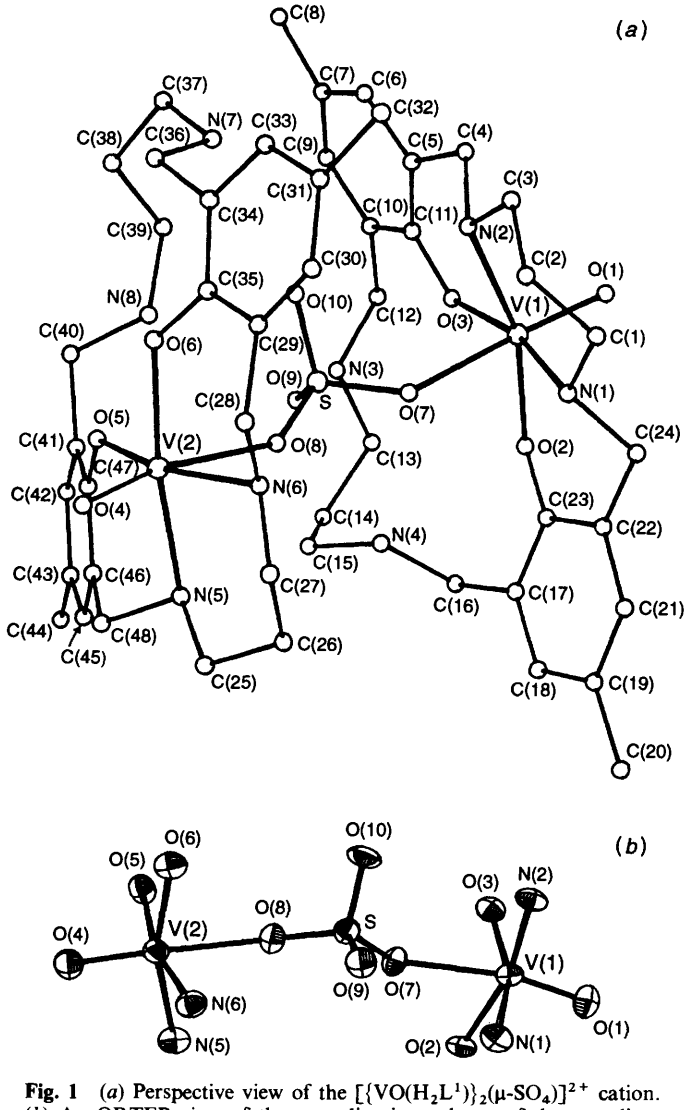

Fig. 1 (*a*) Perspective view of the $[\{VO(H_2L^1)\}_2(\mu\text{-}SO_4)]^{2+}$ cation. (*b*) An ORTEP view of the co-ordination spheres of the vanadium centres

Table 2 Selected bond lengths (Å) and angles (°) for compound **3**

V(1)–O(1)	1.587(9)	V(2)–O(4)	1.600(9)
V(1)–O(2)	1.988(9)	V(2)–O(5)	1.990(9)
V(1)–O(3)	1.974(9)	V(2)–O(6)	1.978(9)
V(1)–O(7)	2.202(9)	V(2)–O(8)	2.236(9)
V(1)–N(1)	2.156(11)	V(2)–N(5)	2.166(11)
V(1)–N(2)	2.170(10)	V(2)–N(6)	2.166(11)
V(1)···V(2)	6.741(4)		
N(1)–V(1)–N(2)	93.5(4)	N(5)–V(2)–N(6)	91.4(4)
O(7)–V(1)–N(2)	79.5(4)	O(8)–V(2)–N(6)	78.8(4)
O(7)–V(1)–N(1)	76.3(4)	O(8)–V(2)–N(5)	80.7(4)
O(3)–V(1)–N(2)	86.3(4)	O(6)–V(2)–N(6)	90.3(4)
O(3)–V(1)–N(1)	166.0(4)	O(6)–V(2)–N(5)	167.9(4)
O(3)–V(1)–O(7)	89.9(4)	O(6)–V(2)–O(8)	87.9(3)
O(2)–V(1)–N(2)	160.9(4)	O(5)–V(2)–N(6)	163.1(4)
O(2)–V(1)–N(1)	87.5(4)	O(5)–V(2)–N(5)	89.1(4)
O(2)–V(1)–O(7)	82.2(4)	O(5)–V(2)–O(8)	84.6(4)
O(2)–V(1)–O(3)	88.3(4)	O(5)–V(2)–O(6)	85.9(4)
O(1)–V(1)–N(2)	95.9(4)	O(4)–V(2)–N(6)	92.2(4)
O(1)–V(1)–N(1)	91.7(4)	O(4)–V(2)–N(5)	90.4(4)
O(1)–V(1)–O(7)	166.8(4)	O(4)–V(2)–O(8)	167.1(4)
O(1)–V(1)–O(3)	102.3(4)	O(4)–V(2)–O(6)	101.5(4)
O(1)–V(1)–O(2)	103.1(4)	O(4)–V(2)–O(5)	104.7(4)

V=O stretching of this compound is observed at 955 cm^{-1}. Freshly prepared solutions of **3** in methanol or methanol–acetonitrile mixture remain clear for several hours. This indicates that solvolytic cleavage into **1** and **2** does not occur because **1** being insoluble would have immediately precipitated.

When compound **2** is treated with 1 equivalent of $[Ni(acac)_2]$ a purple non-electrolyte of composition $[(VO)L^1Ni(H_2O)_2(SO_4)]\cdot H_2O$ **4** is obtained. On the other hand, the reaction between **1** and nickel(II) sulfate affords a violet compound **5** also of the same composition. The two compounds show differences in their IR spectra. For example, for **4** the ν(NH) band occurs at 3260 cm^{-1}, while for **5** this band is observed at 3240 cm^{-1}. More importantly, the V=O stretching frequency of **4** is shifted to a considerably higher energy (975 cm^{-1}) relative to that of **5** (950 cm^{-1}). Moreover, $\nu_3(SO_4^{2-})$ is more split in **5** (1230, 1180, 1120, 1060 and 990 cm^{-1}) as compared to **4** (1180 and 1060 cm^{-1}). These observations suggest that in **4** the sulfate is monodentate and bound to the oxovanadium(IV), while in **5** the two metal centres are bridged by the sulfate.

Electronic spectra

For vanadyl(IV) complexes it is generally considered that transitions occur from d_{xy} to (d_{yz}, d_{xz}) (ν_1), $d_{x^2-y^2}$ (ν_2) and d_{z^2} (ν_3) orbitals with increasing energies.[12] In the visible range **3** exhibits two absorption maximum at 820 and 525 nm which can be attributed to the ν_1 and ν_2 bands of oxovanadium(IV). The third intense band at 295 nm is probably due to a oxo→vanadium(IV) charge-transfer transition admixed with the $d_{xy} \longrightarrow d_{z^2}$ transition. It may be mentioned that the ν_1 and ν_2 bands of **2** also occur[2] at 820 and 520 nm with molar absorption coefficients approximately half those of **3**, indicating that the co-ordination environment of vanadium in the two compounds must be very similar.

The difference in the nature of the sulfate binding in the $Ni^{II}VO^{IV}$ complexes **4** and **5** is clearly seen in their electronic spectra. Complex **4** exhibits bands at 1140, 780, 520 and 295 nm, of which, while that at 1140 nm is evidently due to a $^3A_{2g} \longrightarrow {}^3T_{2g}$ transition of octahedral nickel(II), the remaining three can be reasonably attributed to transitions occurring at the vanadium(IV) centre. It seems likely that the energies of the $^3A_{2g} \longrightarrow {}^3T_{1g}(F)$ and $^3A_{2g} \longrightarrow T_{1g}(P)$ transitions of the nickel(II) are not very different from those of the $d_{xy} \longrightarrow d_{yz}$, d_{zx} and $d_{xy} \longrightarrow d_{x^2-y^2}$ transitions of the oxovanadium(IV). In contrast to **4**, complex **5** exhibits bands at 1120, 710, 680, 570,

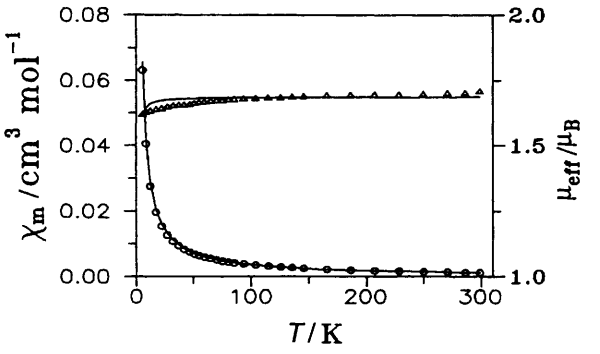

Fig. 2 Plots of molar magnetic susceptibility per vanadium χ_m (○) and effective magnetic moment per vanadium μ_{eff} (△) *vs.* temperature for compound **3**. The solid lines result from a least-squares fit by the theoretical equation (1) given in the text

470 and 350 nm. The occurrence of a larger number relative to that of **4** indicates lower symmetries for the metal centres in **5**. We tentatively assign the five bands at 1120, 710, 570, 470 and 350 nm to the spin-allowed transitions of nickel(II) with a distorted six-fold geometry[12,13] from $^3B_{1g}$ to ^3E_g, $^3B_{2g}$, $^3A_{2g}$, ^3E_g and $^3A_{2g}$ and/or $^3E_g(P)$, respectively. The bands at 680 and 470 nm are probably due to $d_{xy} \longrightarrow d_{yz}$, d_{zx} and $d_{xy} \longrightarrow d_{x^2-y^2}$ transitions of oxovanadium(IV).

Crystal structure

$[\{VO(H_2L^1)\}_2(\mu\text{-}SO_4)][NO_3)_2]$ 3. A perspective view of the complex cation and an ORTEP[14] representation of the co-ordination spheres of the metal atoms in **3** are shown in Fig. 1(*a*) and 1(*b*), respectively. Selected bond distances are given in Table 2. The structure consists of two mononuclear $VO(H_2L^1)$ units joined through the sulfate moiety. Each vanadium atom is co-ordinated to the secondary amine nitrogens and two phenolate oxygens, which provide the equatorial plane, and a distorted octahedral configuration is obtained through the axial co-ordination of an oxo oxygen and bridging sulfate oxygen. The extent of distortion from an ideal octahedral geometry is reflected in the cisoid [76.3(4)–104.7(4)°] and the transoid angles [160.9(4)–167.9(4)°]. The V=O distances [1.587(9) and 1.600(9) Å] are similar to those reported in compounds of related structures.[1,2,11] The metrical parameters for the two vanadium centres indicate that they are very similar but not identical; the differences are seen more in the bond angles than the distances. The in-plane V–O and V–N distances [average 1.983(9) and 2.165(11) Å, respectively] are normal, however the V–O (sulfate) distances [2.202(9) and 2.236(9) Å] are significantly long due to the *trans* influence of the vanadyl group. Atoms V(1) and V(2) are displaced from their corresponding N_2O_2 basal planes toward vanadyl oxygen by 0.295(2) and 0.256(2) Å, respectively. The dihedral angle between the mean planes is 21.1°. The sulfate has normal tetrahedral geometry [average S–O 1.468(18) Å and O–S–O 110.2(14)°], while disorder in some of the oxygen atoms of the nitrate ions affects the N–O bond lengths, which range between 1.12 and 1.29 Å. As shown in Fig. 1(*b*) the two oxovanadium moieties are *trans* with respect to each other and the vanadium atoms are separated by 6.741(4) Å. The molecular structure of **3** reveals the presence of at least ten fairly strong hydrogen bonds,* of which seven are intramolecular. They are mainly between the protonated amines and the oxygen atoms of the sulfate [O(7)–O(10)] or nitrates [O(11)–O(13), O(14)–O(16)]. Interestingly, although there is a hydrogen bond between one of the hydrogens of N(3) and the phenolate oxygen, a similar interaction is absent between N(4) and O(2) or in the counterpart of the second macrocycle.

Magnetic properties and ESR spectra

Dimeric oxovanadium(IV) species generally exhibit antiferromagnetic exchange interaction due to direct overlap of the unpaired electron in the d_{xy} orbital, albeit a few instances of ferromagnetic exchange coupling are known.[15,16] It can be anticipated that the magnitude of the exchange coupling constant (J, where $H = -2JS_1 \cdot S_2$) will rapidly decrease with increasing distance between the two interacting metal centres.[2,17–21] From single-crystal ESR spectra of several mononuclear oxovanadium(IV) complexes it has been shown[22,23] that very weak exchange coupling ($|J|$ *ca.* 0.01–0.02 cm^{-1}) can occur due to intermolecular VO ··· VO interactions even at distances in the range 6–8 Å. In this context it was of interest to examine the magnetic properties of **3** both in the solid state and in solution. It should be noted that, aside from the intramolecular distance of 6.741(4) Å, the two nearest symmetry-related intermolecular V ··· V distances are 7.38 and 8.13 Å.

Variable-temperature magnetic susceptibility measurements of compound **3** have been carried out between 5.2 and 298.9 K. A plot of χ_m^{-1} *vs.* T gave a linear fit with the Weiss constant $\theta = -4.0$ K, indicating that there may be intra- and or inter-molecular exchange interactions. In the entire temperature range there is, of course, a very small but definite change of magnetic moment per vanadium [μ_{eff} decreases from 1.71 (298.9) to 1.64 μ_B (5.2 K)]. However, if the two magnetically equivalent oxovanadium(IV) centres are totally non-interacting then the magnetic moment should remain constant throughout ($\mu_{eff} = 1.71$ μ_B for $g = 1.98$). To account for the observed temperature dependence of μ_{eff} both intra- and inter-molecular exchange interactions have been considered. Assuming an isotropic model, the exchange expression based on the spin Hamiltonian $H = -2JS_1 \cdot S_2 - 2zJ'S^z\langle S^z\rangle$ is given by equation (1). The symbols N, β, g and k have their usual

$$\chi_A = \frac{N\beta^2 g^2 F(J,T)}{kT - 2zJ'F(J,T)} \quad (1)$$

$$F(J,T) = \frac{e^{2J/kT}}{1 + 3e^{2J/kT}} \quad (2)$$

meanings and zJ' refers to the intermolecular exchange interaction. Fig. 2 shows the least-squares fit of the experimental data χ (and μ_{eff}) *vs.* T by equation (1) with $J = -0.1(1)$ cm^{-1}, $zJ' = -0.5(2)$ cm^{-1} and $g = 1.97(1)$. It should be emphasized that the exchange parameters thus obtained are regarded as purely tentative because the susceptibility data are not sufficiently accurate for reliable estimation of such weak interactions.

In the solid state the ESR spectrum of compound **3** at 77 K shows a single-line feature with $g = 1.974$. The fluid solution (MeCN–MeOH) spectrum at room temperature shows an eight-line pattern, typical of a mononuclear oxovanadium(IV) compound (^{51}V, $I = \frac{7}{2}$), with $g_{iso} = 1.976$ and $A_{iso} = 0.0082$ cm^{-1}. Clearly, intramolecular VO ··· VO electron-spin interaction is absent otherwise a fifteen-line hyperfine pattern would have been observed. Further, the frozen-solution spectrum of **3** (Fig. 3) shows the species to be of rhombic symmetry. In the absence of spectral simulation we report only the values of $g_{zz} = 1.964$ and $A_{zz} = 0.0145$ cm^{-1}. It is of interest to compare the ESR spectra of **1**–**3**. As reported earlier,[2] **1** exhibits in the

* The hydrogen bond distances (Å) and angles (°) are: N(3) ··· O(3) 2.94(1), N(3)–H ··· O(3) 133.5(7); N(3) ··· O(9) 2.93(1), N(3)–H ··· O(9) 131.9(7); N(4) ··· O(11) 2.77(2), N(4)–H ··· O(11) 166.0(9); N(4) ··· O(9) 2.90(1), N(4)–H ··· O(9) 125.2(7); N(5) ··· O(11) 3.04(2); N(5)–H ··· O(11) 146.1(7), N(7) ··· O(10) 2.82(1), N(7)–H ··· O(10) 154.7(7); N(8) ··· O(9) 2.80(1), N(8)–H ··· O(9) 143.7(7); N(3) ··· O(14) 2.73(2), N(3)–H ··· O(14) 152.8(8); N(7) ··· O(13) 3.09(8), N(7)–H ··· O(13) 162.0(2); N(7) ··· O(12) 2.89(2), N(7)–H ··· O(12) 146.7(9). The last three interactions are intermolecular.

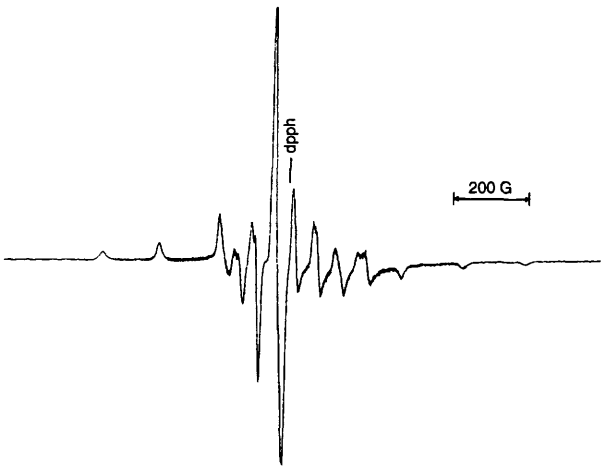

Fig. 3 The ESR spectrum of compound **3** in a MeCN–MeOH frozen glass (77 K). The microwave frequency used was 9.10 GHz; G = 10^{-4} T

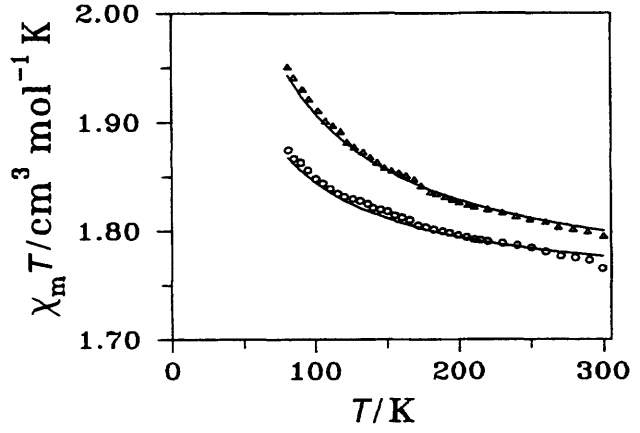

Fig. 4 Plots of $\chi_m T$ *vs.* T for compounds **4** (△) and **5** (○). The solid lines result from a least-squares fit by the theoretical equation (3) given in the text

solid state (77 K) a single-line feature at $g = 1.97$ and a weak resonance at $g = 3.92$ due to a $\Delta M_s = \pm 2$ transition resulting from ··· V=O ··· V=O ··· stacking interactions. On the other hand, the frozen-solution spectrum of **2** has the characteristics of axial symmetry with $g_{\|} = 1.952$, $g_{\perp} = 1.991$, $A_{\|} = 0.0147$ cm^{-1} and $A_{\perp} = 0.0047$ cm^{-1}. Two important points have emerged from the ESR spectroscopic studies. First, the well resolved spectrum of **3** (Fig. 3) rules out its dissociation in solution into **1** and **2**. Secondly, although there is some kind of weak exchange interaction in **3** in the solid state, intramolecular interaction is absent in solution.

Magnetic susceptibility measurements have been made for the heterodinuclear $VO^{IV}Ni^{II}$ complexes **4** and **5** in the limited temperature range 85–300 K. As shown in Fig. 4, the experimental data ($\chi_m T$ *vs.* T) could be least-squares fitted by equation (3) with $J = 10(1)$ cm^{-1} for **4** and 6(1) cm^{-1} for **5**,

$$\chi_m = \frac{N\beta^2 g^2}{kT} \cdot \frac{1 + 10e^{3J/kT}}{4(1 + 2e^{3J/kT})} \qquad (3)$$

keeping g fixed at 2.25. Since both the magnetic orbitals of nickel ($d_{x^2-y^2}$ and d_{z^2}) are orthogonal to that of vanadium (d_{xy}), the observed ferromagnetic behaviour of **4** and **5** is as expected. However, in the absence of their crystal structures the difference in the J values cannot be rationalized. A more definitive magnetostructural relationship in $VO^{IV}M^{II}$ (M = Cu, Ni, Co, Fe or Mn) systems will be reported [24] elsewhere.

Electrochemistry

The electrochemical behaviour of complexes **3**–**5** with regard to their oxidation has been studied by cyclic voltammetry (CV) in MeCN–MeOH (4:1) solutions. As shown in Fig. 5(*a*), **3** undergoes two successive oxidation processes. The first couple ($VO^{IV}VO^{IV}$–$VO^{IV}VO^{V}$) at 0.445 V *vs.* Ag–AgCl is fully reversible ($\Delta E_p = 60$ mV), while the second ($VO^{IV}VO^{V}$–$VO^{V}VO^{V}$) at 0.60 V is nearly reversible ($\Delta E_p = 85$ mV, scan rate $v = 100$ mV s^{-1}). In the case of the first couple all three criteria of reversibility, *viz.* (*i*) linear variation of peak current with $v^{\frac{1}{2}}$, (*ii*) unity ratio of cathodic and anodic currents and (*iii*) anodic and cathodic separation (ΔE_p) independent of scan rate (v), have been used to establish its identity. Under similar experimental conditions, for ferrocene $\Delta E_p = 65$ mV and $E_{\frac{1}{2}} = 0.390$ V. The comproportionation constant K_c, obtained from the relation $K_c = 10^{\Delta E_{\frac{1}{2}}/0.0591}$, is 4.2×10^2. It may be mentioned that in molecules containing two chemically equivalent totally non-interacting reversible redox sites the separation between the redox potentials $\Delta E_{\frac{1}{2}}$ will be statistically 35.6 mV,[25] that is for such systems $K_c = 4$. In practice, however, for most commonly observed cases, K_c is greater than 4. For example, in the stepwise reduction as well as oxidation of the dicopper(II)[26] and dinickel(II)[27] complexes of H_2L^1 we have noted that K_c may lie in the range $10^2 - 10^5$. In the case of **3** sequential two-electron transfer was expected, but the occurrence of two closely spaced redox couples ($\Delta E_{\frac{1}{2}} = 0.155$ V) suggests that removal of an electron from the second metal centre is relatively more difficult than the first. A closer examination of the crystallographic data (Table 2) reveals that although the bond lengths for the two vanadium atoms are quite similar, perceptible differences exist in their bond angles. Thus, slight geometrical differences facilitate easier oxidation of one vanadium(IV) centre with respect to the other.

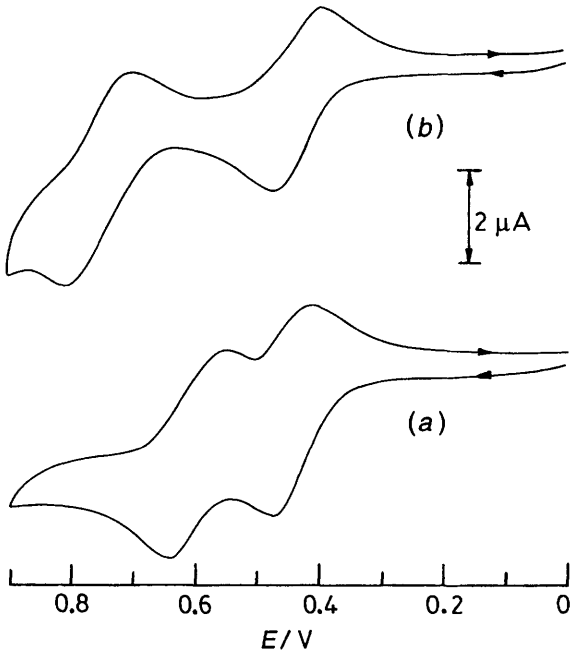

Fig. 5 Cyclic voltammograms of compounds **3** (*a*) and **4** (*b*) in MeCN–MeOH (4:1) solutions at a scan rate (v) of 100 mV s^{-1}

In contrast to compound **3**, the oxidation of **2** takes place quasi-reversibly ($\Delta E_p = 100$–120 mV, $v = 50$–500 mV s^{-1}) at $E_{\frac{1}{2}} = 0.44$ V. The occurrence of two redox couples for **3** as against one for **2** in the potential window 0–1 V provides a clear indication that the structure of **3** is maintained in solution. Taken together, the CV, UV/VIS and ESR measurements have established that although the co-ordination environments, around the vanadium atoms in **2** and **3** are closely similar, the two species retain their separate identity in solution.

The cyclic voltammogram of $[(VO)L^1Ni(H_2O)_2(SO_4)]\cdot H_2O$ **4** in MeCN–MeOH (4:1) solution [Fig. 5(*b*)] also exhibits two reversible redox couples. The first at $E_{\frac{1}{2}} = 0.436$ V ($\Delta E_p = 70$

mV, ν = 100 mV s^{-1}), which is very similar to the first redox couple of **3**, is due to VO^{IV}–VO^{V}, while the second at 0.756 V (ΔE_p = 70 mV) is due to Ni^{II}–Ni^{III}. The electrochemical behaviour of $[(VO)L^1Ni(\mu\text{-}SO_4)(H_2O)]\cdot 2H_2O$ **5** in MeCN is in sharp contrast to that of **4**. In this case both the metal centres are irreversibly oxidized at 1.05 and 1.25 V. The slow heterogeneous electron-transfer rates observed for **5** are in accord with the distorted co-ordination geometries of the metal centres.

Acknowledgements

Financial support from the Department of Science and Technology, Government of India is gratefully acknowledged. We thank Professor L. K. Thompson of Memorial University of Newfoundland, St. John's for variable-temperature magnetic measurements of compound **3**.

References

1 K. K. Nanda, S. Mohanta, S. Ghosh, M. Mukherjee, M. Helliwell and K. Nag, *Inorg. Chem.*, 1995, **34**, 2861.
2 R. Das, K. K. Nanda, A. K. Mukherjee, M. Mukherjee, M. Helliwell and K. Nag, *J. Chem. Soc., Dalton Trans.*, 1993, 2241.
3 P. de Loth, P. Karafiloglou, J. P. Daudey and O. Kahn, *J. Am. Chem. Soc.*, 1988, **110**, 5676.
4 S. K. Mandal and K. Nag, *J. Org. Chem.*, 1986, **51**, 3900.
5 W. C. Fernelius, *Inorg. Synth.*, 1957, **5**, 105.
6 K. K. Nanda, R. Das, L. K. Thompson, K. Venkatsubramanian and K. Nag, *Inorg. Chem.*, 1994, **33**, 5934.
7 A. C. T. North, D. C. Philips and F. S. Mathews, *Acta Crystallogr., Sect. A*, 1968, **24**, 351.
8 G. M. Sheldrick, SHELX 76, Program for Crystal Structure Determination, University of Cambridge, 1976.
9 G. M. Sheldrick, SHELXL 93, Program for Crystal Structure Refinement, University of Göttingen, 1993.
10 *International Tables for X-Ray Crystallography*, Kluwer Academic Publishers, Dordrecht, 1992, vol. C.
11 S. Ghosh, M. Mukherjee, A. K. Mukherjee, S. Mohanta and M. Helliwell, *Acta Crystallogr., Sect. C*, 1994, **50**, 1204.
12 A. B. P. Lever, *Inorganic Electronic Spectroscopy*, 2nd edn., Elsevier, Amsterdam, 1984.
13 K. K. Nanda, R. Das, M. J. Newlands, R. Hynes, E. J. Gabe and K. Nag, *J. Chem. Soc., Dalton Trans.*, 1992, 897.
14 C. K. Johnson, ORTEP II, Report ORNL-3794, revised, Oak Ridge National Laboratory, Oak Ridge, TN, 1971.
15 R. L. Belford, N. D. Chasteen and R. E. Tapscott, *J. Am. Chem. Soc.*, 1969, **91**, 4675.
16 C. W. Hahn, P. G. Rasmussen and J. C. Bayon, *Inorg. Chem.*, 1992, **31**, 1963.
17 A. Neves, K. Wieghardt, B. Nuber and J. Weiss, *Inorg. Chim. Acta*, 1988, **150**, 183.
18 M. Koppen, G. Fresen, K. Wieghardt, R. M. Llusar, B. Nuber and J. Weiss, *Inorg. Chem.*, 1988, **27**, 721.
19 K. Wieghardt, V. Bossek, K. Volckmar, W. Swiridoff and J. Weiss, *Inorg. Chem.*, 1984, **23**, 1387.
20 D. Collison, D. R. Eardley, F. E. Mabbs, A. K. Powell and S. S. Turner, *Inorg. Chem.*, 1993, **32**, 664.
21 S. L. Castro, M. E. Cass, F. J. Hollander and S. L. Bartley, *Inorg. Chem.*, 1995, **34**, 466.
22 G. D. Simpson, R. L. Belford and R. Biagioni, *Inorg. Chem.*, 1978, **17**, 2424.
23 B. Gahan and F. E. Mabbs, *J. Chem. Soc., Dalton Trans.*, 1983, 1695, 1713; D. Collison, B. Gahan and F. E. Mabbs, *J. Chem. Soc., Dalton Trans.*, 1983, 1705.
24 S. Mohanta, K. K. Nanda, L. K. Thompson, U. Flörke and K. Nag, unpublished work.
25 D. E. Richardson and H. Taube, *Coord. Chem. Rev.*, 1984, **60**, 107.
26 S. K. Mandal, L. K. Thompson, K. Nag, J.-P. Charland and E. J. Gabe, *Inorg. Chem.*, 1987, **26**, 1391.
27 R. Das and K. Nag, *Inorg. Chem.*, 1991, **30**, 2831.

Received 29*th April* 1996; *Paper* 6/02975B